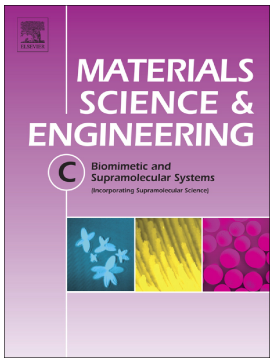

Self-assembly of glucose oxidase on reduced graphene oxide-magnetic nanoparticles nanocomposite-based direct electrochemistry for reagentless glucose biosensor

Saithip Pakapongpan, Rungtiva P. Poo-arporn

PII: S0928-4931(16)31251-6
DOI: doi: 10.1016/j.msec.2017.03.031
Reference: MSC 7539

To appear in: *Materials Science & Engineering C*

Received date: 9 September 2016
Revised date: 11 January 2017
Accepted date: 3 March 2017

Please cite this article as: Saithip Pakapongpan, Rungtiva P. Poo-arporn , Self-assembly of glucose oxidase on reduced graphene oxide-magnetic nanoparticles nanocomposite-based direct electrochemistry for reagentless glucose biosensor. The address for the corresponding author was captured as affiliation for all authors. Please check if appropriate. Msc(2017), doi: 10.1016/j.msec.2017.03.031

Self-assembly of glucose oxidase on reduced graphene oxide-magnetic nanoparticles nanocomposite-based direct electrochemistry for reagentless glucose biosensor

Saithip Pakapongpan[a,b] and Rungtiva P.Poo-arporn[a,*]

[a] Biological Engineering Program, Faculty of Engineering, King Mongkut's University of Technology Thonburi, Bangkok 10140, Thailand

[b] Thailand Organic and Printed Electronics Innovation Center, National Electronics and Computer Technology Center, NSTDA, Pathum Thani 12120, Thailand

E-mail: rungtiva.pal@kmutt.ac.th

Corresponding authors Tel.: +66 2 4709393

Abstract

A novel approach of the immobilization of a highly selective and stable glucose biosensor based on direct electrochemistry was fabricated by a self-assembly of glucose oxidase (GOD) on reduced graphene oxide (RGO) covalently conjugated to magnetic nanoparticles (Fe_3O_4 NPs) modified on a magnetic screen-printed electrode (MSPE). The RGO-Fe_3O_4 nanocomposite has remarkable enhancement in large surface areas, is favorable environment for enzyme immobilization, facilitates electron transfer between enzymes and electrode surfaces and possesses superparamagnetism property. The morphology and electrochemical properties of RGO-Fe_3O_4/GOD were characterized by scanning electron microscopy (SEM), Fourier transform infrared spectroscopy (FTIR), Raman spectroscopy, cyclic voltammetry (CV) and amperometry. The modified electrode was a fast, direct electron transfer with an apparent electron transfer rate constant (k_s) of 13.78 s^{-1}. The proposed biosensor showed fast amperometric response (3 s) to glucose with a wide linear range from 0.05 to 1 mM, a low detection limit of 0.1 μM at a signal to noise ratio of 3 (S/N=3) and good sensitivity (5.9 μA/mM). The resulting biosensor has high stability, good reproducibility, excellent selectivity and successfully applied detection potential at –0.45 V. This mediatorless glucose sensing used the advantages of covalent bonding and self-assembly as a new approach for immobilizing enzymes without any binder. It would be worth noting that it opens a new avenue for fabricating excellent electrochemical biosensors.

Keywords: Reduced graphene oxide; Direct electrochemistry; Glucose biosensor; Magnetic nanoparticles

1. Introduction

Blood glucose level is usually used as a clinical indicator of diabetes mellitus, which is a global health problem with devastating social and economic impact [1]. Moreover, the determination of glucose concentration is also very important in food processing and fermentation. An electrochemical biosensor is a potential tool and more suitable for point of care devices than normal conventional methods including spectrophotometry [2], HPLC [3], fluorescence [4] and chemiluminescence [5]. Glucose oxidase (GOD) modified electrodes have played a leading role in highly selective blood sugar testing by electrochemical method. GOD is one of the most extensively researched enzymes for the construction of enzyme-based glucose biosensors. Since it contains two flavin adenine dinucleotide (FAD) cofactors as a redox center [6], direct electron transfer (DET) between redox enzymes and the surface of electrodes can be used to investigate enzyme-catalyzed reactions in biological systems and electrochemical basis for the study of the structure, kinetics and thermodynamics of redox transformations of enzyme molecules and metabolic processes involving redox transformations [7-9]. However, the FAD redox centers in protein molecules are usually embedded deeply into the large structure of an enzyme. Thus, it is extremely difficult to observe the direct electrochemistry of GOD with a conventional electrode. Great effort has been made to develop new mediator-free biosensors and biomedical devices based on DET by immobilizing enzymes on conducting substrates in order to improve the electron transfer between the redox centers of GOD and the surface of an electrode. Several methods and nanomaterials including polymers [10], gold nanoparticles [11], sol–gel matrices [12] and nanocomposites [13] have been studied to immobilize enzymes which can improve the long-term stability of biosensor applications. Additionally, nanomaterials can significantly improve the electroactivity of bioelectrodes because they provide a more efficient electrical contact with the enzymes' active sites, an optimal environment for the immobilization of

proteins and other biological molecules, and provide a larger surface area that enables incorporation of larger enzyme loading. Carbon based nanostructures have been reported for the immobilization of enzymes in the fabrication of biosensors such as carbon nanotubes [8], nanoparticles [13, 14] and graphene [15] which can offer direct and fast electron transport to electron collecting electrodes. In particular, graphene have been proven to be a versatile and tunable material compared to other materials.

Graphene possesses many unique features such as a large surface area, good electrical conductivity, and thermal and mechanical properties. The unique properties make graphene widely employed for various applications such as field-effect transistors [16], gas sensors [17, 18], electromechanical sensors-biosensors [19-21], nanoelectronics [22], batteries [23, 24], supercapacitors [25] and hydrogen storage [26]. In addition, varieties of hybrid materials between graphene and other materials such as polymers, metals, metal oxides and even carbon nanotubes with new functions look promising to be used in varieties of applications. Immobilization of bioactive molecules on the surface of magnetic nanoparticles is of great interest, because the magnetic behavior of these bioconjugates is likely to improve and recovery of biomolecules for biomedical applications [27]. Fe_3O_4 NPs as special bimolecular immobilizing carriers are becoming the focus in many applications [28, 29] due to good biocompatibility, strong superparamagnetic, low toxicity, large surface-to-volume ratio, high surface reaction activity, and strong adsorption ability to immobilize desired biomolecules in an easy preparation process [30]. Therefore, the integration of RGO and Fe_3O_4 NPs into a hybrid material with enzymes could afford hybrid nanobiomaterials with synergistic properties, provide more surface area, offer good biocompatibility for enzymes immobilized, and enhance functionalities improving electric contact with enzyme active sites and electrode surfaces; thus, the electron transfer distance will be decreased and then facilitate this process. As previously reported, [31], it has been shown that RGO-Fe_3O_4 NPs modified glassy carbon

electrodes showed direct electrochemistry of GOD with the physical absorption immobilized method. The method is simple but this kind of Fe_3O_4 attachment may easily leach out from the RGO resulting in the stability of biosensors being rather poor.

In this work, the novel, simple and low cost strategy to develop a disposable glucose biosensor based on direct electrochemistry will be purposed. We used a nanocomposite between the RGO and Fe_3O_4 NPs with GOD to increase the immobilization of an enzyme, enhance the sensitivity and selectivity and especially improve the stability of the electrode without a binder. Due to Fe_3O_4 NPs being surrounded by a positive charge, they play an important role in immobilizing enzymes through electrostatic interaction. GOD is a negatively charged biomolecule at pH 7.0 [32] that can be easily immobilized onto the positively charged amino group on an Fe_3O_4 NPs surface via electrostatic interaction. The RGO-Fe_3O_4 nanocomposite was prepared by covalent bonding via coupling agent, EDC and NHS, and immobilized enzymes by electrostatic interaction, which is extremely strong. This might be advantageous over physical absorption. The properties of the RGO and Fe_3O_4 NPs provide biosensors more efficient conductivity and increase the immobilization of enzymes. Moreover, this proposed reagentless glucose sensor combines the excellent properties of MSPE (low cost, mass produced, portable, miniaturized, disposable sensor enabled) with the advantages of the RGO-Fe_3O_4 nanocomposite which not only has a great potential to increase the immobilization of the enzymes but also could be used to attracted enzymes onto electrode surfaces with a strong magnetic force. The nanocomposite was investigated by the electrochemical performance of a glucose biosensor by cyclic voltammetry and amperometry. This biosensor platform might be used in medical devices applications for point of care devices in the future.

2. Experimental section

2.1. Reagents and materials

Graphene oxide (GO > 99 wt% purity and total thickness < 3nm. Average dimensions of individual flakes range from 300-800 nm, Glucose oxidase (EC 1.1.3.4 from Aspergillus niger, 210,000 U/g) Iron (III) chloride hexahydrate ($FeCl_3.6H_2O$), 1-ethyl-3-(3-dimethyaminopropyl) carbodiimide (EDC), N-hydroxysuccinimide (NHS), Ammonium hydroxide (NH_4OH), 1,6-Hexanediamine, Glucose, Sodium acetate (NaAc), Ethylene glycol (EG) was purchased from Sigma Aldrich and used without further purification. A 0.1 M phosphate buffer saline (PBS, pH 7.0) was prepared by mixing solutions of Na_2HPO_4 and NaH_2PO_4. The glucose solution was prepared overnight before use to allow the mutarotation for 24 hours. All solutions were prepared with deionized water (DI).

2.2. Apparatus

All electrochemical experiments were performed with a potentiostat (Metrohm Autolab PGSTAT302N, Ecochemie, Netherlands) in a conventional three-electrode electrochemical cell using a magnetic screen-printed electrode (MSPE) as a working electrode, a platinum electrode as a counter electrode and an Ag/AgCl saturated KCl as the reference electrode.

2.3 Magnetic screen-printed electrode fabrication

The magnetic screen-printed electrode (MSPE) was prepared by a rectangular magnet sticker (1.5 x 2 mm) put onto the backside of a screen-printed electrode (SPE).

2.4. Preparation of RGO-Fe_3O_4 nanocomposite modified electrode

The NH_2-Fe_3O_4 NPs were prepared through a solvothermal reaction according to F. Zhang et al. 2011 [33]. The Fe_3O_4 NPs was immobilized on GO using EDC and NHS as coupling agents by the formation of an amide link between the amino group of Fe_3O_4 NPs and the carboxyl group of GO. 20 mg GO in 60 mL water was ultrasonicated for 3 h, and then 100 mg EDC and 80 mg NHS were added into the solution of GO. The mixture was stirred for 30 min and ultrasonicated for another 30 min to form a homogenous suspension.

Next, 20 mg of NH_2-Fe_3O_4 NPs was added into the suspension solution and the mixture was subjected to ultrasonication for 30 min. The reaction was carried out at 80 °C for 1 h under stirring. The GO-Fe_3O_4 nanocomposite was obtained by magnetic separation and washed with water several times.

An RGO-Fe_3O_4 nanocomposite based on glucose reduction was prepared. In brief, 40 mg glucose was added into a 25 mL GO-Fe_3O_4 dispersion solution followed by stirring for more than 0.5 h. and 20 µl ammonia solution (25% w/w) was added into the resulting dispersion solution. After being stirred for a few minutes, the mixture was again stirred for 60 min at 95 °C. Finally, the resulting stable black dispersion solution was centrifuged and washed with water several times. The obtained RGO-Fe_3O_4 nanocomposite (1 mg/2.5 mL) was redispersed in DI water before further use. Finally, the 5 µl RGO-Fe_3O_4 nanocomposite solution was dropped onto the MSPE surface.

2.5. Preparation of RGO-Fe_3O_4/GOD nanocomposite modified electrode

GOD was immobilized onto the RGO-Fe_3O_4 nanocomposite modified MSPE through an electrostatic interaction between positive charges of Fe_3O_4 and negative charges of GOD. 30 mg GOD was added into 1 mL 0.1 M PBS pH 7.0 solution. The RGO-Fe_3O_4 nanocomposite modified MSPE was immersed into the GOD solution (30 mg/mL in 0.1 M PBS pH 7.0), and then reacted at room temperature for 12 h. The RGO-Fe_3O_4/GOD nanocomposite modified electrode surface was washed with DI water to remove unadsorbed enzyme molecules and allowed to dry at room temperature. The modified electrode was stored at 4 °C when not in use. The fabrication process is shown in Scheme 1.

3. Results and Discussion

3.1. Characterization of RGO-Fe_3O_4/GOD nanocomposite

The surface morphology of GO characterized by SEM is shown in Fig. 1a. A few layers of GO sheets appear partially packed with their basal planes, intensely crumpled and folded

into a typical wrinkled structure. These geometric wrinkling and rippling were caused by nanoscale interlocking of GO sheets. The spherical Fe_3O_4 NPs were clearly observed as shown in Fig. 1b and distributed well on the whole surface of a RGO sheet due to the strong interaction of covalent bond (Fig. 1c). The diameter of Fe_3O_4 NPs was about 32 nm. In Fig. 1d, after the immobilization of GOD on the RGO-Fe_3O_4 nanocomposite by electrostatic force, the nanocomposite showed deposition of a protein globular structure on the uniform structure and the roughness increased dramatically indicating that the enzymes were successfully immobilized on the surface of the Fe_3O_4 NPs and the size of particles was slightly increased. The results confirm the preparation of the nanocomposite.

3.2. Fourier transform infrared (FT-IR) study of RGO-Fe_3O_4 nanocomposite

The GO-Fe_3O_4 nanocomposite was obtained from the NHS and EDC and the condensation reaction between the amino group of Fe_3O_4 NPs and carboxylic group of GO which formed a carboxamide bonding. The confirmation of binding between the GO and Fe_3O_4 NPs was studied by FT-IR spectroscopy. The FT-IR spectra of the NH_2-Fe_3O_4 NPs (curve a), GO (curve b), and GO-Fe_3O_4 nanocomposite (curve c) are shown in Fig. 2A. The band of NH_2-Fe_3O_4 NPs, as shown in curve a, was found at 571 cm^{-1}, which corresponded to the Fe–O stretching vibration, and the two spectrum bands observed at 1630 and 3351 cm^{-1} were assigned to the N–H bending and stretching vibrations of free amino groups on the Fe_3O_4 NPs as reported [34]. The results indicated that the amino group has been grafted onto the Fe_3O_4 NPs surface. Fig. 2A curve b shows the FT-IR spectrum of GO, and a strong and broad absorption at 3401 cm^{-1} was observed, which was due to the O–H stretching vibration. The absorptions' peak at 1724 and 1375 cm^{-1} corresponded to the C=O stretching of carboxylic acid and carbonyl moieties. For the aromatic C=C and the epoxy group, alkoxy C–O, stretching vibrations were observed at 1625 and 1084 cm^{-1}, respectively [35]. In curve

c, after introducing the Fe_3O_4 NPs on GO, the FT-IR spectrum of the GO-Fe_3O_4 appeared in the band at 565 cm^{-1} and illustrated the Fe–O stretching vibration, confirming the deposition of Fe_3O_4 on GO. Three new characteristic peaks of the amide carbonyl group for GO-Fe_3O_4 nanocomposite at 1634 (–CONH amide band I), 1544 (–NH amide band II), and 1368 cm^{-1} (C–N stretch of amide) appeared, implying that Fe_3O_4 NPs were successfully linked to the GO sheet via covalent bonding after the amidation reaction [36]. The two bands at 3284 and 1634 cm^{-1} were attributed to the O–H stretching vibration, and to the N–H stretching vibrations and the NH_2 bending mode of the free NH_2 group, respectively. However, the GO-Fe_3O_4 nanocomposite is still composed of functional groups with an oxygen component such as hydroxyl and ether groups on both sides. Glucose was applied as a reducing agent to remove oxygen components. The FT-IR spectra of GO-Fe_3O_4 nanocomposite and RGO-Fe_3O_4 nanocomposite are presented in Fig. 2B, curves a and b, respectively. In the GO-Fe_3O_4 spectrum, the graph shows the stretching of hydroxyl group at 3284 cm^{-1}(O–H stretching), the C=O carbonyl stretching at 1634 cm^{-1} and 1718 cm^{-1}, as well as the C−O epoxide group stretching at 1060 cm^{-1}. All these bands related with the oxygen-containing functional groups mostly remain in the FT-IR spectrum of the GO-Fe_3O_4 nanocomposite. The high intensity of the main peaks in the GO-Fe_3O_4 nanocomposite confirmed the presence of a large number of oxygen functional groups as shown in Fig. 2B curve a. After the GO was chemically reduced, the characteristic absorption bands of hydroxyl at 3168 cm^{-1} were significantly decreased. The carbonyl group at 1554 cm^{-1} and 1368 cm^{-1}, and alkoxy groups at 1060 cm^{-1} in curve b disappeared, indicating the high efficiency of reduction and oxygen-containing functional groups' removal from the GO. The absorption band that appears at 1629 cm^{-1} may be attributed to the skeletal vibration of the graphene sheets [37]. Moreover, observing an additional peak can be ascribed to the lattice absorption of Fe_3O_4 NPs at 572 cm^{-1}. These confirmed that most of the oxygen-containing functional groups were already removed.

3.3. Raman spectroscopy study of RGO-Fe_3O_4 nanocomposite

Raman spectroscopy was used to investigate the electronic structure of graphene and characterize the reduction degree of the GO. The Raman spectroscopies of the GO, GO-Fe_3O_4 and RGO-Fe_3O_4 are shown in Fig. 3. Typically, the Raman spectrum of graphene was characterized by two fundamental vibrations the G band corresponds to the first order scattering of the E2g phonon of sp^2 C atoms (usually observed at ~1575 cm^{-1}), a characteristic band of crystalline graphite, and the D band indicates the reduction in size of the in-plane sp^2 domains for the chemical oxidation of graphite (~1350 cm^{-1}) [37, 38]. In the Raman spectrum of the GO (curve a), the G band is broadened and blue shifts to 1597 cm^{-1}, which is attributed to the presence of isolated double bonds that resonate at higher frequencies than the G band of graphite. The D band at 1358 cm^{-1} becomes prominent, indicating the reduction in size of the in-plane sp^2 domains due to the extensive oxidation. As shown in Fig. 3 curve c, the Raman spectrum of the RGO-Fe_3O_4 exhibits D and G at 1346 and 1594 cm^{-1}, and the G band of RGO-Fe_3O_4 moves to 1594 cm^{-1}, which is closer to that of graphite, indicating the GO was reduced. The intensity ratio of the D to G peak (I_D/I_G) is found to change inversely with graphitic domain size and widely used to study the crystalline quality of graphite or graphene after the treatment. The I_D/I_G improved from the GO was 0.83, GO-Fe_3O_4 (0.89) to RGO-Fe_3O_4 (1.03). This change suggested that more sp^2 domains are formed during the reduction of graphite oxide. This increase is due to the decrease of the sp^2 in-plane domain induced by the introduction of defects and disorder of the sp^2 domain.

3.4. Direct electrochemistry of GOD immobilized RGO-Fe_3O_4 modified electrode

The electrochemical properties of nanocomposite were studied using cyclic voltammetry. Under appropriate conditions, the DET between the GOD and the substrate can be observed from the electrochemical response. Fig. 4A shows the cyclic voltammograms of

GOD-modified different electrodes in the N_2-saturated PBS at a scan rate of 100 mV/s. No redox peaks were observed for the GOD/MSPE (curve a) and Fe_3O_4-GOD/MSPE (curve b). The background current of the Fe_3O_4-GOD/MSPE was higher than that of the GOD/MSPE, and is ascribed to the large surface area of the Fe_3O_4, which showed a distinct electrochemical response. Fig. 4A, curve c showed a well-defined redox peak with an anodic peak potential (E_{pa}) at –0.418 V and a cathodic peak potential (E_{pc}) at –0.452 V. The peak potential separation (ΔE_p) was about 34 mV. These results demonstrated a fast DET kinetics of the GOD on the surface of the Fe_3O_4 on the graphene sheet. The well-defined and quasi-reversible redox peaks suggested a favorable DET between the electrode and the redox centers of the GOD molecules. The formal potential ($E^{0'}$) obtained by averaging the potential values of the E_{pa} and E_{pc} was –0.435 V. This value was close to the standard electrode potential of –0.483 (vs. Ag/AgCl) for FAD/$FADH_2$ at pH 7.0 [39], suggesting that the GOD molecules retain their bioactivity after the adsorption on the RGO-Fe_3O_4 nanocomposite, and the electrochemistry response of the GOD immobilized on the modified electrode is due to the redox reaction of the FAD.

3.5. The influence of the scan rate

The effect of the scan rate on the cyclic voltammetric performance at the RGO-Fe_3O_4/GOD modified MSPE with different scan rates is shown in Fig. 4B, where the redox processes of the nanocomposite gave mostly symmetric anodic and cathodic peaks (E_{pa} and E_{pc}) at relatively slow scan rates. When the scan rate increased, the redox potentials of the GOD shifted slightly. The anodic and cathodic peak currents (I_{pa}, I_{pc}) linearly increased with the increasing scan rate from 10 to 100 mV/s, indicating that the redox reaction of the GOD on the RGO-Fe_3O_4 modified electrode was a quasi-reversible surface-controlled process. The plot of the cathodic peak current versus the scan rate showed a linear relationship (Fig. 4C)

with linear regression equations: I_{pa} = 0.0153x+0.0383, I_{pc} = –0.0149x–0.0475 with a correlation coefficient (R^2) of 0.993 and 0.992, respectively. These results demonstrated a fast DET kinetics of the GOD on the surface of the graphene.

According to Laviron's equation [40], the plots of the E_{pa} and E_{pc} versus the logarithm of the scan rates produced two straight lines with slopes of $2.3RT/(1–\alpha)nF$ and $–2.3RT/\alpha nF$ at high scan rates (up to 1000 mV/s) as shown in Fig. 4D. The charge transfer coefficient (α) and the heterogeneous electron transfer rate constant (k_s) for the proposed electrode were calculated to be 0.5 and 13.78 s^{-1}, respectively, according to the following equation:

$$\log k_s = \alpha \log(1-\alpha) + (1-\alpha)\log\alpha - \log\frac{RT}{nFv} - \frac{\alpha(1-\alpha)nF\Delta E_p}{2.3RT} \quad (1)$$

Where R is gas constant, T is temperature, v is scan rate and ΔE_p is peak separation. This result confirmed that the RGO-Fe_3O_4 facilitated the fast electron transfer between the redox-active site of enzyme and the surface of the electrode. These results suggest that the RGO-Fe_3O_4/GOD provides fast electron transfer kinetics between the redox center of the enzyme and the surface of the electrode. The superior electron transfer kinetics of graphene can be ascribed to their unique electronic structures, which are favorable for conducting electrons from the redox center to the electrode surface. The surface average concentration of GOD (Γ, mol/cm^2) on the electrode can be calculated from the charge integration of the cathodic peak in the cyclic voltammogram according to the formula, $\Gamma = Q/nFA$, where Q is the charge consumed in C, n is the number of electrons transferred (n=2 for DET of GOD), A is the electrode area (cm^2) and F is the faraday constant. The electroactive GOD concentration on the RGO-Fe_3O_4 was estimated to be 4.95×10^{-11} mol/cm^2, indicating a saturated adsorption of the GOD the onFe_3O_4 surface of the nanocomposite which is higher than previously reported at a GOD on a mesoporous iron oxide modified SPE [41].

3.6. The influence of solution pH

It is well known that the direct electrochemistry of a GOD has a two-electron coupled with two-proton reaction. Therefore, the pH value of the solution should have an effect on the electrochemical behavior of the GOD on the RGO-Fe_3O_4, and a negative shift of both the cathodic and anodic peak potentials occurs when the solution's pH value was increased as shown in Fig. 5A. The redox potential $E^{0'}$ changes linearly as a function of the solution pH from 4 to 9 with a slope of –52 mV/pH (r^2 = 0.9989). This slope is close to the theoretical value of –58.6 mV/pH [42] according to the reaction of equation (2) for a reversible reaction, indicating two protons ($2H^+$) and two electrons ($2e^-$) attending in the electron transfer process. The reaction mechanism can be written as follows:

$$GOD\ (FAD) + 2e^- + 2H^+ \leftrightarrow GOD\ (FADH_2) \qquad (2)$$

3.7. Electrocatalytic activity of the RGO-Fe_3O_4/GOD/MSPE to glucose

In order to study the enzymatic catalytic activity of the GOD adsorbed on the RGO-Fe_3O_4/MSPE, the experiments were carried out by cyclic voltammetry. Fig. 5B shows the CVs of the RGO-Fe_3O_4/GOD/MSPE with different glucose concentration in 0.1 M PBS pH 7.0 at the scan rate of 30 mV s^{-1}. Under N_2-saturated condition (curve g), a pair of well-defined and almost symmetrical redox peaks was observed, which indicates that a GOD adsorbed on an RGO-Fe_3O_4/MSPE can undergo a reversible direct electrochemical reaction, and this implies the DET of the GOD for $FADH_2$ oxidation and FAD reduction in equation (2). In O_2-saturated condition (curve a), the reduction peak current of the RGO-Fe_3O_4/GOD/MSPE was larger than that in the N_2-saturated PBS and the oxidation peak current was smaller. The reason for this is that the GOD ($FADH_2$) was oxidized to regenerate the oxidized form of the GOD (FAD) because O_2 is a natural co-substrate for the GOD. It confirms that oxygen dissolved in the PBS solution was reduced at the electrode according to

the following equations (3) which was a typical electrochemical catalytic process, in which oxygen regenerates the GOD (FAD) and enhances the reduction peak current of the FAD. When glucose was added into this system (curve b-f), the GOD reacted with the glucose and turned FAD into the reduced form of the GOD ($FADH_2$) as shown in equation (4). Fig. 5B, curve b-f shows the CVs of the RGO-Fe_3O_4/GOD/MSPE with various concentrations of glucose. It was found that the reduction peak currents decrease with increasing glucose concentration ranging from 0.05 mM to 10 mM due to the enzyme-catalyzed reaction that occurred and the decrease of the FAD form concentration at the electrode surface, indicating that the GOD retains its high bioelectrocatalytic activity to the glucose. The results were consistent with the previous reports [43]. Therefore, based on the decrease of the reduction current, the concentration of glucose can be detected and used as a biosensor system for reagentless glucose sensing. The electrocatalytic mechanism can be expressed as follows:

$$\text{GOD } (FADH_2) + O_2 \rightarrow \text{GOD } (FAD) + H_2O_2 \quad (3)$$

$$\text{GOD } (FAD) + \text{Glucose} \rightarrow \text{GOD } (FADH_2) + \text{Gluconolactone} \quad (4)$$

3.8. Amperometric response of the glucose biosensor

From the relationship between the decrease of the reduction current and the concentration of glucose, the amperometry technique was used to perform at the applied potential of –0.45 V in 0.1 M PBS pH 7.0. Fig. 6A shows typical steady-state amperometric responses of the RGO-Fe_3O_4/GOD/MSPE on successive injections of glucose under stirring. The steady-state current obtained on the RGO-Fe_3O_4/GOD/MSPE decreased during the addition of glucose concentration. The electrocatalytic response was very fast as the biosensor achieved the maximum response after 3 s when glucose was added into the solution. As the inset of Fig 6A, the resulting calibration plot is presented over the concentration range 0.05 to 1.2 mM. It was found that the reduction current response

decreased with increasing proportional to the glucose concentration. The plot of current response vs. glucose concentration was linear in the ranges of 0.05 to 1 mM with the linear regression equation of y = 5.873x + 0.131 (correlation coefficient 0.993) and a sensitivity of 5.9 μA/mM. The detection limit was calculated to be 0.1 μM at a signal-to-noise ratio of 3 (S/N=3). The comparison of the analytical performance of the developed electrode with some other previous reports on direct glucose biosensors are summarized in Table 1. It can be seen that this biosensor exhibits a lower detection limit and a higher sensitivity compared with other Fe_3O_4 electrodes and SPE based glucose biosensors. Typically, the DET was extremely difficult to occur at SPE more than at GCE because of the lower sensitivity and surface area. The presence of the Fe_3O_4 and graphene could increase the conductivity of the electrode and the GOD could quickly transfer electrons to electrodes. The resulting good performance was not only due to the strong bonding but the paramagnetism force might reduce the spacing of enzymes and increase the amount of nanocomposites to entrap into the porous SPE surface.

The apparent Michaelis-Menten constant (K_M^{app}) values were evaluated by an electrochemical Lineweaver-Burk equation [44, 45] which can provide an indication of the enzyme–substrate kinetics.

$$\frac{1}{I_{ss}} = \frac{1}{I_{\max}} + \frac{K_M^{app}}{I_{ss}} \cdot \frac{1}{C} \qquad (5)$$

Here, I_{ss} is the steady-state current, C the concentration of substrate, and I_{max} the maximum current response. The corresponding plot yielded an "apparent" K_m of 0.16 mM. The value was smaller than those reported for the DET of the GOD [31, 46-48] indicating that it has a higher affinity towards glucose. The good microenvironment due to the synergistic effect of the nanocomposite might contribute to the improvement of the affinity and good performances of the biosensor.

3.9. Repeatability and stability of the RGO-Fe_3O_4/GOD/MSPE

The reproducibility of the biosensor was investigated by the amperometric method. The relative standard deviation (RSD) was calculated to be 3.98%, which was determined by 5 different modified electrodes of 0.5 mM glucose. The result demonstrates that the reproducibility and precision of the sensor was good. The stability was tested by measuring the decrease in the cyclic voltammetric current during potential cycling in 0.1 M PBS pH 7.0. The peak height and peak potential of the immobilized enzyme on RGO-Fe_3O_4 remained nearly unchanged and the amount of the GOD remaining on the electrode surface was almost 98.4% of its initial value after 50 cycles (Fig. S1). Furthermore, the long term stability of the biosensor exhibited a current response that retention of 95.6% after being stored at 4ºC for 1 month which indicated that the nanocomposite modified electrode had high long term stability due to the strong covalent attachment of RGO-Fe_3O_4 and electrostatic attraction of GOD onto the electrode surface, preventing enzymes from leaking out of the electrode surface.

3.10. Interference study

Common interference in blood such as ascorbic acid (AA), uric acid (UA), and dopamine (DA) usually coexist with glucose in human blood, which can interfere with the current signal. The direct electrochemistry of the GOD could avoid the interferences in the procedure of detecting glucose. The normal physiological level of glucose is 3 to 8 mM, which is much higher than those of the interfering species of AA (~0.1 mM) and UA (~0.02 mM). The amperometric current responses of the RGO-Fe_3O_4/GOD/MSPE to the addition of 0.1 mM UA, 1 mM AA, 1 mM DA and 0.5 mM glucose at the applied potentials of –0.45 V

in 0.1 M PBS pH 7.0 were evaluated. As can be seen in Fig. 6B, the interference was not observed. It can prove the selectivity of this biosensor.

4. Conclusions

We have successfully prepared an RGO-Fe_3O_4/GOD nanocomposite modified MSPE by covalent bonding and a GOD was self-assembled with an RGO-Fe_3O_4 applied to it for constructing a mediatorless glucose biosensor. An RGO-Fe_3O_4/GOD nanocomposite can provide a unique microenvironment for direct electrochemistry of a GOD immobilized on the surface of a modified electrode, which can retain its high electrocatalytic activities. This can be attributed to the following: (1) the covalent bonding of Fe_3O_4 on a graphene sheet and electrostatic interaction between enzymes on the RGO-Fe_3O_4 which enhance the contact and reduce the spacing of the electrode and redox center of an enzyme, (2) the high conductivity of graphene which promotes the electron transfer rate, (3) this modified electrode did not use a binder and adhesive agent that usually block electron transfers at electrode surfaces, and (4) the use of Fe_3O_4 NPs not only increases the surface area but also has paramagnetic properties which makes them easily manipulated by an external magnetic field to prevent the leaching of enzymes at electrode surfaces. Moreover, the SPE has the advantages of miniaturization, mass production and low cost, thus it is very useful in a disposable measurement for point of care devices. The nanocomposite shows an excellent electrocatalytic activity, high selectivity, sensitivity, wide range and low detection limit. This biosensor fabrication could be applied for other applications of several analytes in clinical diagnosis, pharmaceutical analysis and in the field of bio-electrochemistry.

Acknowledgments

This work was supported by the Thailand Research Fund (TRF) and the Synchrotron Light Research Institute (SLRI) (grant number RSA5980073), the Research Strengthening Project of the Faculty of Engineering, King Mongkut's University of Technology Thonburi, the Higher Education Research Promotion and the National Research University Project of Thailand, Office of the Higher Education Commission. S. Pakapongpan would like to express her gratitude for the Researcher Career Development Grant from National Research Council of Thailand (NRCT).

References

[1] A. Heller, B. Feldman, Electrochemical glucose sensors and their applications in diabetes management, Chemical reviews, 108 (2008) 2482-2505.

[2] H. Heise, R. Marbach, G. Janatsch, J. Kruse-Jarres, Multivariate determination of glucose in whole blood by attenuated total reflection infrared spectroscopy, Analytical chemistry, 61 (1989) 2009-2015.

[3] A. Wilson, T. Work, A. Bushway, R. Bushway, HPLC determination of fructose, glucose, and sucrose in potatoes, Journal of Food Science, 46 (1981) 300-301.

[4] R.J. Russell, M.V. Pishko, C.C. Gefrides, M.J. McShane, G.L. Cote, A fluorescence-based glucose biosensor using concanavalin A and dextran encapsulated in a poly (ethylene glycol) hydrogel, Analytical Chemistry, 71 (1999) 3126-3132.

[5] X. Liu, E.H. Hansen, Sequential injection determination of D-glucose by chemiluminescence using an open tubular immobilised enzyme reactor, Analytica chimica acta, 326 (1996) 1-12.

[6] H. Hecht, H. Kalisz, J. Hendle, R. Schmid, D. Schomburg, Crystal structure of glucose oxidase from Aspergillus niger refined at 2·3 Å reslution, Journal of molecular biology, 229 (1993) 153-172.

[7] J.E. Frew, H.A.O. Hill, Direct and indirect electron transfer between electrodes and redox proteins, European Journal of Biochemistry, 172 (1988) 261-269.

[8] C. Cai, J. Chen, Direct electron transfer of glucose oxidase promoted by carbon nanotubes, Analytical biochemistry, 332 (2004) 75-83.

[9] F.A. Armstrong, H.A.O. Hill, N.J. Walton, Direct electrochemistry of redox proteins, Accounts of Chemical Research, 21 (1988) 407-413.

[10] X. Kang, J. Wang, H. Wu, I.A. Aksay, J. Liu, Y. Lin, Glucose oxidase–graphene–chitosan modified electrode for direct electrochemistry and glucose sensing, Biosensors and Bioelectronics, 25 (2009) 901-905.

[11] H. Zhang, Z. Meng, Q. Wang, J. Zheng, A novel glucose biosensor based on direct electrochemistry of glucose oxidase incorporated in biomediated gold nanoparticles–carbon nanotubes composite film, Sensors and Actuators B: Chemical, 158 (2011) 23-27.

[12] O. Nadzhafova, M. Etienne, A. Walcarius, Direct electrochemistry of hemoglobin and glucose oxidase in electrodeposited sol–gel silica thin films on glassy carbon, Electrochemistry Communications, 9 (2007) 1189-1195.

[13] Z. Luo, L. Yuwen, Y. Han, J. Tian, X. Zhu, L. Weng, L. Wang, Reduced graphene oxide/PAMAM–silver nanoparticles nanocomposite modified electrode for direct electrochemistry of glucose oxidase and glucose sensing, Biosensors and Bioelectronics, 36 (2012) 179-185.

[14] A. Salimi, E. Sharifi, A. Noorbakhsh, S. Soltanian, Immobilization of glucose oxidase on electrodeposited nickel oxide nanoparticles: Direct electron transfer and electrocatalytic activity, Biosensors and Bioelectronics, 22 (2007) 3146-3153.

[15] P. Wu, Q. Shao, Y. Hu, J. Jin, Y. Yin, H. Zhang, C. Cai, Direct electrochemistry of glucose oxidase assembled on graphene and application to glucose detection, Electrochimica Acta, 55 (2010) 8606-8614.

[16] F. Xia, D.B. Farmer, Y.-m. Lin, P. Avouris, Graphene field-effect transistors with high on/off current ratio and large transport band gap at room temperature, Nano letters, 10 (2010) 715-718.

[17] G. Ko, H.-Y. Kim, J. Ahn, Y.-M. Park, K.-Y. Lee, J. Kim, Graphene-based nitrogen dioxide gas sensors, Current Applied Physics, 10 (2010) 1002-1004.

[18] H.J. Yoon, J.H. Yang, Z. Zhou, S.S. Yang, M.M.-C. Cheng, Carbon dioxide gas sensor using a graphene sheet, Sensors and Actuators B: Chemical, 157 (2011) 310-313.

[19] T. Kuila, S. Bose, P. Khanra, A.K. Mishra, N.H. Kim, J.H. Lee, Recent advances in graphene-based biosensors, Biosensors and Bioelectronics, 26 (2011) 4637-4648.

[20] M. Pumera, A. Ambrosi, A. Bonanni, E.L.K. Chng, H.L. Poh, Graphene for electrochemical sensing and biosensing, TrAC Trends in Analytical Chemistry, 29 (2010) 954-965.

[21] Y. Shao, J. Wang, H. Wu, J. Liu, I.A. Aksay, Y. Lin, Graphene based electrochemical sensors and biosensors: a review, Electroanalysis, 22 (2010) 1027-1036.

[22] C. Berger, Z. Song, T. Li, X. Li, A.Y. Ogbazghi, R. Feng, Z. Dai, A.N. Marchenkov, E.H. Conrad, P.N. First, Ultrathin epitaxial graphite: 2D electron gas properties and a route toward graphene-based nanoelectronics, The Journal of Physical Chemistry B, 108 (2004) 19912-19916.

[23] M. Liang, L. Zhi, Graphene-based electrode materials for rechargeable lithium batteries, Journal of Materials Chemistry, 19 (2009) 5871-5878.

[24] G. Wang, X. Shen, J. Yao, J. Park, Graphene nanosheets for enhanced lithium storage in lithium ion batteries, Carbon, 47 (2009) 2049-2053.

[25] J.J. Yoo, K. Balakrishnan, J. Huang, V. Meunier, B.G. Sumpter, A. Srivastava, M. Conway, A.L. Mohana Reddy, J. Yu, R. Vajtai, Ultrathin planar graphene supercapacitors, Nano letters, 11 (2011) 1423-1427.

[26] L. Wang, K. Lee, Y.-Y. Sun, M. Lucking, Z. Chen, J.J. Zhao, S.B. Zhang, Graphene oxide as an ideal substrate for hydrogen storage, ACS nano, 3 (2009) 2995-3000.

[27] J. He, M. Huang, D. Wang, Z. Zhang, G. Li, Magnetic separation techniques in sample preparation for biological analysis: A review, Journal of pharmaceutical and biomedical analysis, 101 (2014) 84-101.

[28] C.H. Dodd, H.-C. Hsu, W.-J. Chu, P. Yang, H.-G. Zhang, J.D. Mountz, K. Zinn, J. Forder, L. Josephson, R. Weissleder, Normal T-cell response and in vivo magnetic resonance imaging of T cells loaded with HIV transactivator-peptide-derived superparamagnetic nanoparticles, Journal of immunological methods, 256 (2001) 89-105.

[29] M. Arruebo, R. Fernández-Pacheco, M.R. Ibarra, J. Santamaría, Magnetic nanoparticles for drug delivery, Nano today, 2 (2007) 22-32.

[30] Y. Jiang, C. Guo, H. Xia, I. Mahmood, C. Liu, H. Liu, Magnetic nanoparticles supported ionic liquids for lipase immobilization: Enzyme activity in catalyzing esterification, Journal of Molecular Catalysis B: Enzymatic, 58 (2009) 103-109.

[31] L. Yu, H. Wu, B. Wu, Z. Wang, H. Cao, C. Fu, N. Jia, Magnetic Fe_3O_4-Reduced Graphene Oxide Nanocomposites-Based Electrochemical Biosensing, Nano-Micro Letters, 6 (2014) 258-267.

[32] G. Liu, Y. Lin, Amperometric glucose biosensor based on self-assembling glucose oxidase on carbon nanotubes, Electrochemistry Communications, 8 (2006) 251-256.

[33] F. Zhang, J. Jin, X. Zhong, S. Li, J. Niu, R. Li, J. Ma, Pd immobilized on amine-functionalized magnetite nanoparticles: a novel and highly active catalyst for hydrogenation and Heck reactions, Green Chemistry, 13 (2011) 1238-1243.

[34] H. Ni, X. Sun, Y. Li, C. Li, Solvothermal self-assembly of magnetic Fe_3O_4 nanochains by ethylenediamine functionalized nanoparticles for chromium (VI) removal, Journal of Materials Science, 50 (2015) 4270-4279.

[35] S. Bahar, F. Karami, Amino-functionalized Fe_3O_4–graphene oxide nanocomposite as magnetic solid-phase extraction adsorbent combined with flame atomic absorption spectrometry for copper analysis in food samples, Journal of the Iranian Chemical Society, 12 (2015) 2213-2220.

[36] F. He, J. Fan, D. Ma, L. Zhang, C. Leung, H.L. Chan, The attachment of Fe_3O_4 nanoparticles to graphene oxide by covalent bonding, Carbon, 48 (2010) 3139-3144.

[37] C. Zhu, S. Guo, Y. Fang, S. Dong, Reducing sugar: new functional molecules for the green synthesis of graphene nanosheets, ACS nano, 4 (2010) 2429-2437.

[38] Z.-J. Fan, W. Kai, J. Yan, T. Wei, L.-J. Zhi, J. Feng, Y.-m. Ren, L.-P. Song, F. Wei, Facile synthesis of graphene nanosheets via Fe reduction of exfoliated graphite oxide, ACS nano, 5 (2010) 191-198.

[39] Y. Liu, M. Wang, F. Zhao, Z. Xu, S. Dong, The direct electron transfer of glucose oxidase and glucose biosensor based on carbon nanotubes/chitosan matrix, Biosensors and Bioelectronics, 21 (2005) 984-988.

[40] E. Laviron, General expression of the linear potential sweep voltammogram in the case of diffusionless electrochemical systems, Journal of Electroanalytical Chemistry and Interfacial Electrochemistry, 101 (1979) 19-28.

[41] J. Yu, J. Tu, F. Zhao, B. Zeng, Direct electrochemistry and biocatalysis of glucose oxidase immobilized on magnetic mesoporous carbon, Journal of Solid State Electrochemistry, 14 (2010) 1595-1600.

[42] Q. Liu, X. Lu, J. Li, X. Yao, J. Li, Direct electrochemistry of glucose oxidase and electrochemical biosensing of glucose on quantum dots/carbon nanotubes electrodes, Biosensors and Bioelectronics, 22 (2007) 3203-3209.

[43] K.H. Hyun, S.W. Han, W.-G. Koh, Y. Kwon, Fabrication of biofuel cell containing enzyme catalyst immobilized by layer-by-layer method, Journal of Power Sources, 286 (2015) 197-203.

[44] F. Shu, G. Wilson, Rotating ring-disk enzyme electrode for surface catalysis studies, Analytical Chemistry, 48 (1976) 1679-1686.

[45] Z.O. Araci, A.F. Runge, W.J. Doherty, S.S. Saavedra, Correlating molecular orientation distributions and electrochemical kinetics in subpopulations of an immobilized protein film, Journal of the American Chemical Society, 130 (2008) 1572-1573.

[46] L. Yang, X. Ren, F. Tang, L. Zhang, A practical glucose biosensor based on Fe_3O_4 nanoparticles and chitosan/nafion composite film, Biosensors and Bioelectronics, 25 (2009) 889-895.

[47] T.-H. Yang, C.-L. Hung, J.-H. Ke, J.-M. Zen, An electrochemically preanodized screen-printed carbon electrode for achieving direct electron transfer to glucose oxidase, Electrochemistry Communications, 10 (2008) 1094-1097.

[48] H.-P. Peng, R.-P. Liang, L. Zhang, J.-D. Qiu, Facile preparation of novel core–shell enzyme–Au–polydopamine–Fe_3O_4 magnetic bionanoparticles for glucose sensor, Biosensors and Bioelectronics, 42 (2013) 293-299.

[49] S. Zuo, Y. Teng, H. Yuan, M. Lan, Direct electrochemistry of glucose oxidase on screen-printed electrodes through one-step enzyme immobilization process with silica sol–gel/polyvinyl alcohol hybrid film, Sensors and Actuators B: Chemical, 133 (2008) 555-560.

[50] J. Li, R. Yuan, Y. Chai, Simple construction of an enzymatic glucose biosensor based on a nanocomposite film prepared in one step from iron oxide, gold nanoparticles, and chitosan, Microchimica Acta, 173 (2011) 369-374.

[51] C. Karuppiah, S. Palanisamy, S.-M. Chen, V. Veeramani, P. Periakaruppan, Direct electrochemistry of glucose oxidase and sensing glucose using a screen-printed carbon electrode modified with graphite nanosheets and zinc oxide nanoparticles, Microchimica Acta, 181 (2014) 1843-1850.

Figure captions

Scheme 1. Schematic illustration of RGO-Fe_3O_4/GOD modified MSPE

Fig. 1. SEM images of (a) GO, (b) Fe_3O_4 NPs, (c) RGO-Fe_3O_4 nanocomposite and (d) RGO-Fe_3O_4/GOD nanocomposite.

Fig. 2. FT-IR spectra of (A) NH_2-Fe_3O_4 NPs(a), GO (b), GO-Fe_3O_4 nanocomposite (c), (B) FT-IR spectra of GO-Fe_3O_4 nanocomposite (a) and RGO-Fe_3O_4 nanocomposite (b).

Fig. 3. Raman spectra of GO (a), GO-Fe_3O_4 (b) and RGO-Fe_3O_4 (c).

Fig. 4. (A) Cyclic voltammograms of the different modified electrodes with GOD/MSPE (a), Fe_3O_4/GOD/MSPE (b) and RGO-Fe_3O_4/GOD/MSPE (c) in 0.1 M PBS pH 7.0 with N_2-saturated at a scan rate of 100 mV/s. (B) CVs of the RGO-Fe_3O_4/GOD/MSPE in 0.1 M PBS pH 7.0 at different scan rates inner to outer: 10, 20, 30, 40, 50, 60, 70, 80 and 100 mV/s. (C) The relationship of the peak current (I_p) vs. the scan rates. (D) The relationship of the peak potential (E_p) vs. the logarithm of scan rates (log v).

Fig. 5. (A) CVs of the RGO-Fe_3O_4/GOD/MSPE in 0.1 M PBS with different pH values of 4, 5, 6, 7, 8 and 9 at a scan rate of 50 mV/s. (B) CVs of RGO-Fe_3O_4/GOD/MSPE in 0.1 M PBS pH 7.0 at a scan rate of 30 mV/s in the presence of various concentrations of glucose (a) O_2-saturated without glucose and with glucose concentration of 0.5 (b), 1 (c), 4 (d), 8 (e) and 10 mM (f) and N_2-saturated without glucose (g).

Fig. 6. Amperometric response of (A) RGO-Fe_3O_4/GOD/MSPE to successive addition of glucose concentration at applied potential of –0.45 V in 0.1 M PBS pH 7.0. Inset is the calibration curve for glucose obtained at the biosensor. (B) RGO-Fe_3O_4/GOD/MSPE to 1 mM UA, 1 mM AA, 0.5 mM glucose and 1 mM DA at the applied potential of –0.45 V in 0.1 M PBS pH 7.0.

Table 1 Comparison of analytical performance of DET glucose biosensors based Fe_3O_4 and SPE.

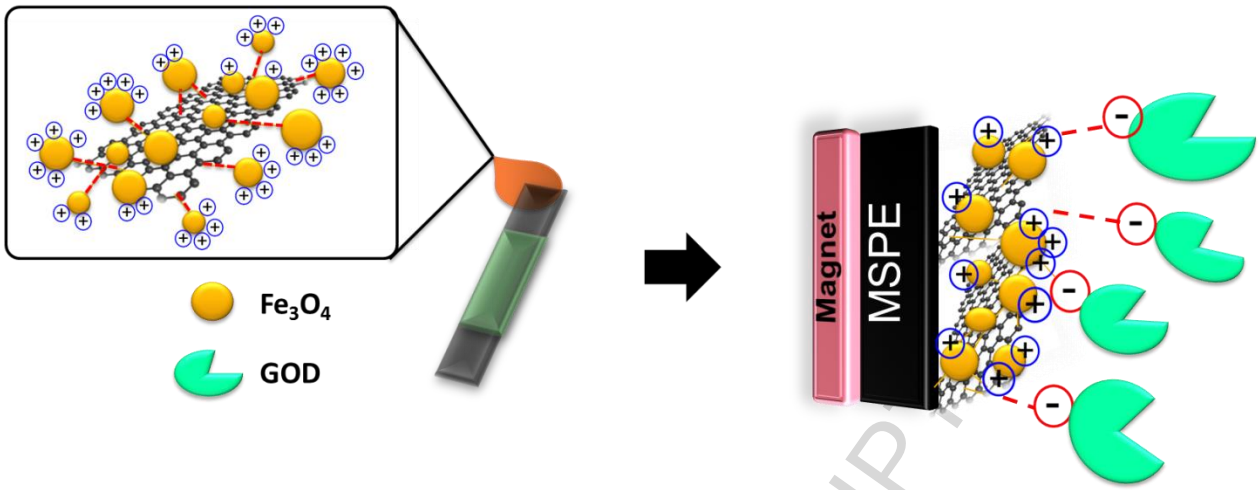

Scheme 1.

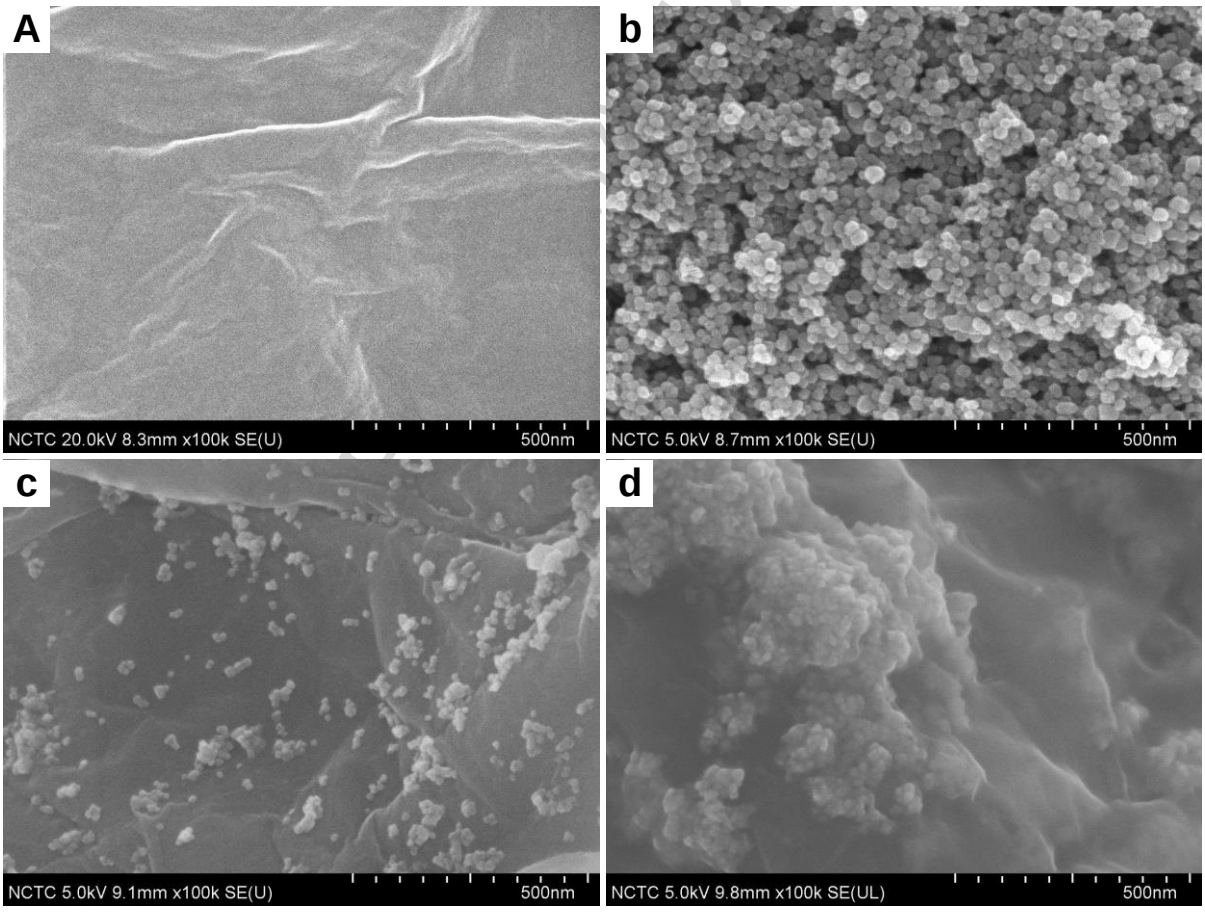

Fig. 1.

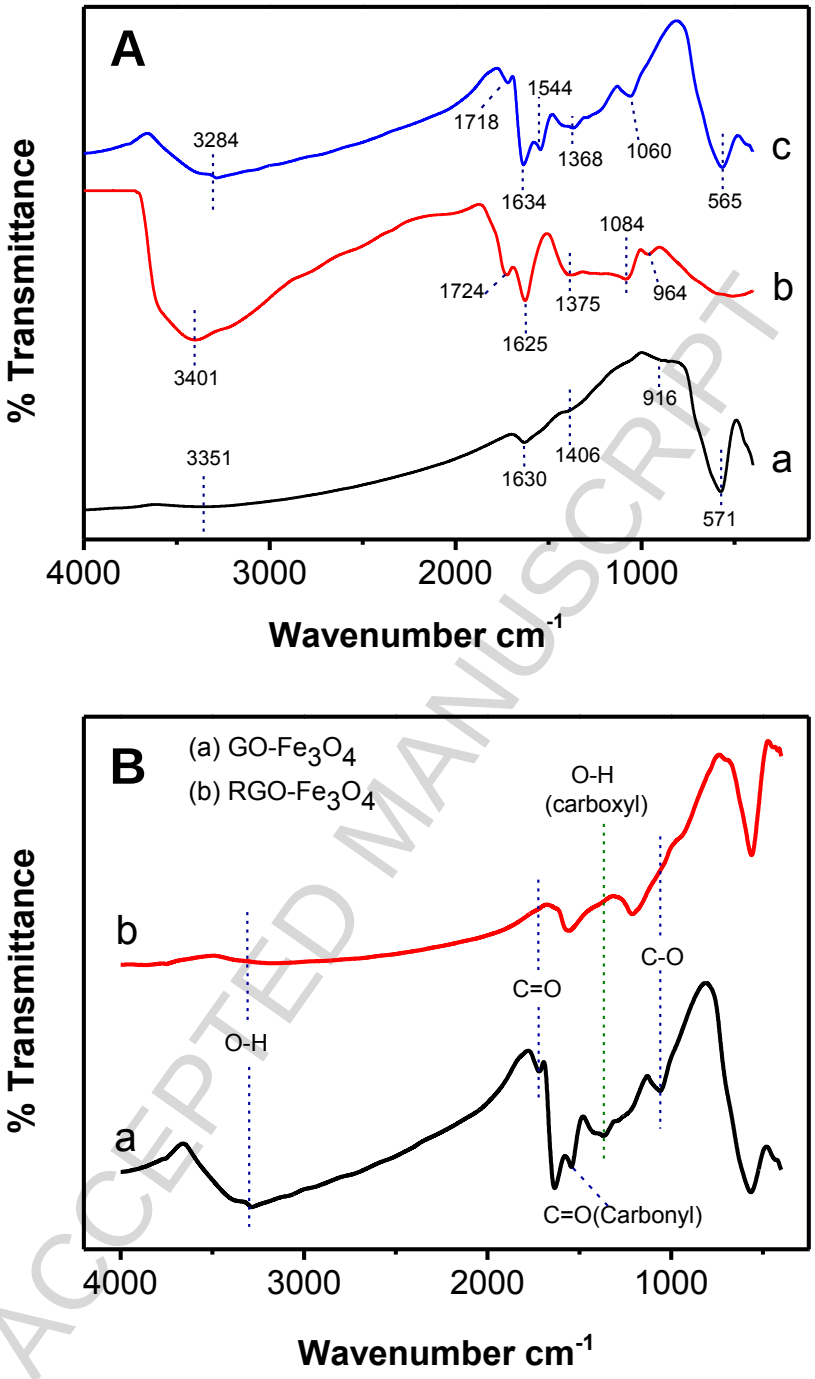

Fig. 2.

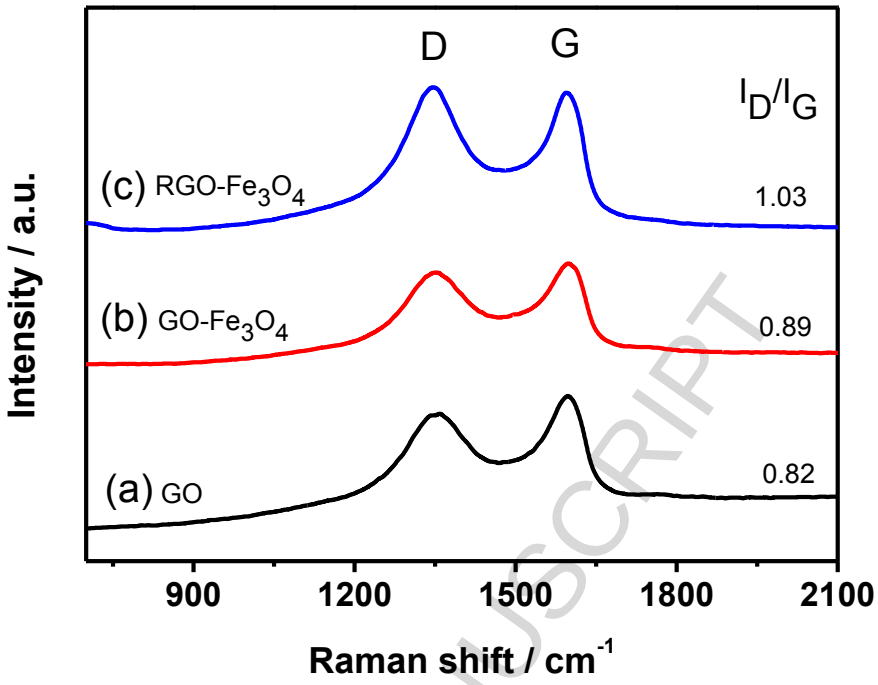

Fig. 3.

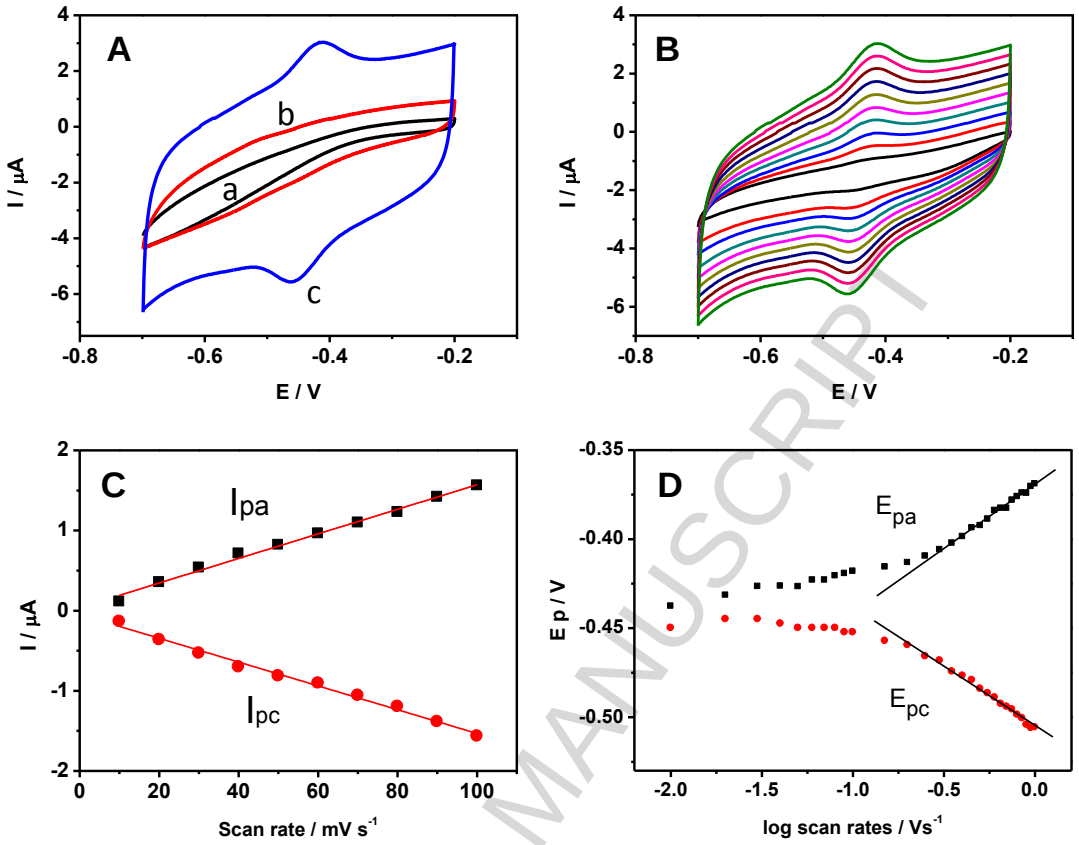

Fig. 4.

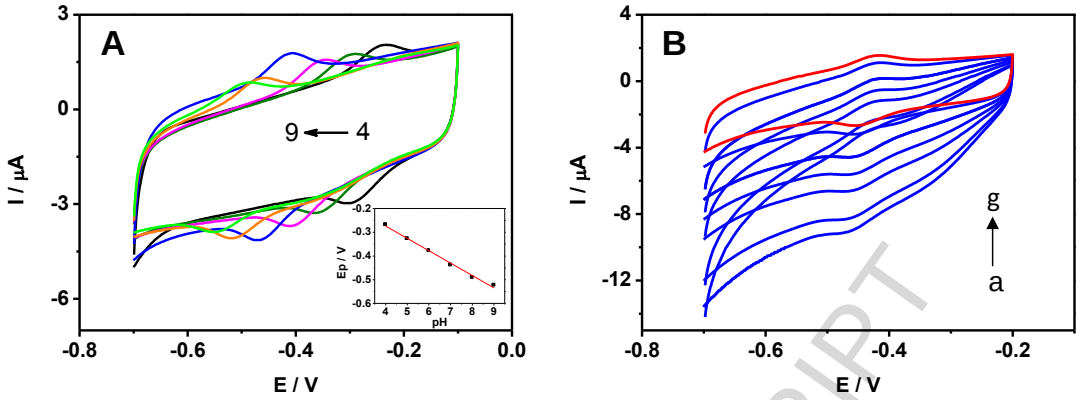

Fig. 5.

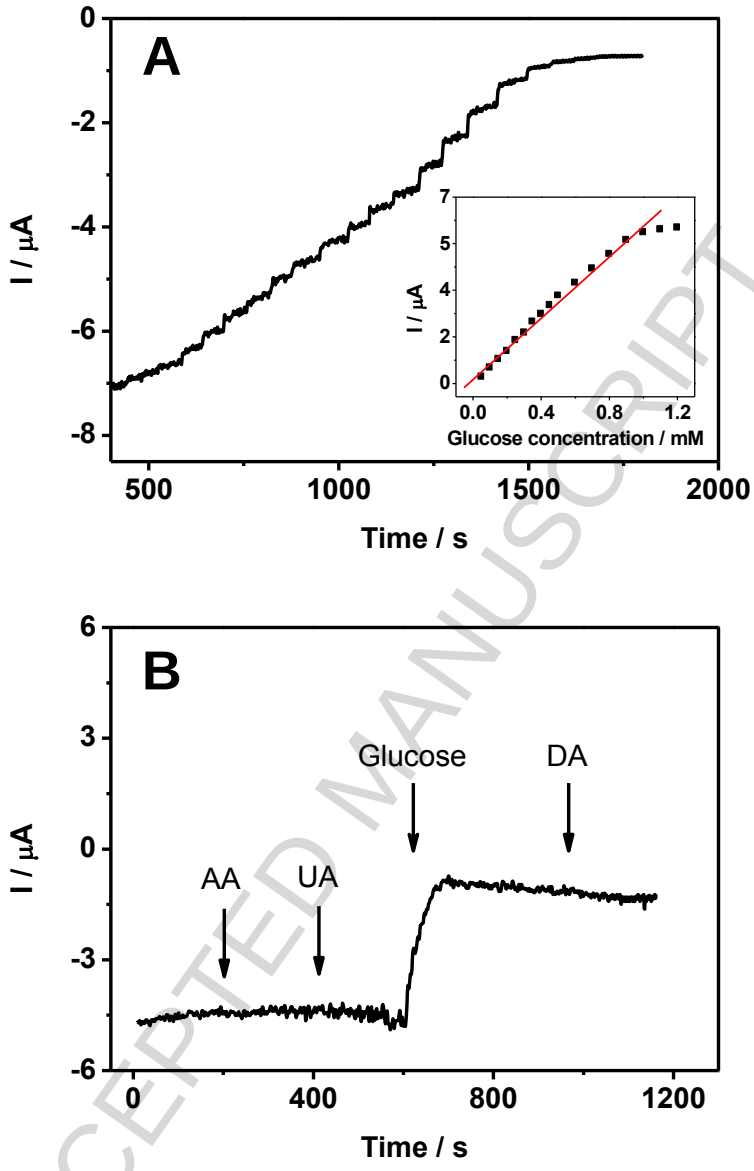

Fig. 6.

Table 1 Comparison of analytical performance of DET glucose biosensors based Fe_3O_4 and SPE.

Modified electrodes	k_s(s^{-1})	Linear range (mmol l^{-1})	LOD (μmol l^{-1})	Immobilized method	K_m (mM)	Ref.
Silica sol-gel/PVA/SPE	8.38	0 - 4.13	9.8	Sol-gel	-	[49]
Nafion/preanodized SPE	4.38	0.1 - 0.9	-	Polymer entrapment	1.07	[47]
Fe_3O_4-AuNPs-CS/AuE	-	0.003 - 0.57	1.2	Polymer entrapment	-	[50]
AuNPs-PDA-Fe_3O_4/MGCE	3.8	0.02 - 1.875	6.5	Polymer entrapment	1.67	[48]
GNs/ZnO/SPE	3.75	0.3 - 4.5	70	Physical Absorption	-	[51]
RGO-Fe_3O_4/MGCE	3.4	0.05 - 1.5	0.15	Physical Absorption	0.34	[31]
RGO-Fe_3O_4/MSPE	13.78	0.05 - 1	0.1	Covalent, electrostatic	0.16	This work

RGO: reduced graphene oxide
GCE: glassy carbon electrode
PVA: polyvinyl alcohol
AuNPs: gold nanoparticles
PDA: poly (dopamine)
MGCE: magnetic glassy carbon electrode
GNs: graphite nanosheets
ZnO: zinc oxide nanoparticles
AuE: gold electrode
CS: chitosan

Novelty Statement

This is a new approach that reporting the immobilization of glucose oxidase on reduced graphene oxide (RGO) covalently conjugated to magnetic nanoparticles (Fe_3O_4 NPs) by electrostatic interaction and modified screen printed electrode. We propose the reagentless with fabrication method without binder and adhesive agents for immobilized enzyme. Fe_3O_4 NPs increasing surface area to enhance the immobilization and prevent the leaching of enzymes at electrode surfaces by magnetic stickers which is improve the stability of the biosensor. Based on this synthesis technique, it is a good new strategy and simple used to fabrication of third-generation glucose biosensor and this nanocomposite could be used as a platform for disposable biosensor and biofuel cell applications.

Graphical Abstract

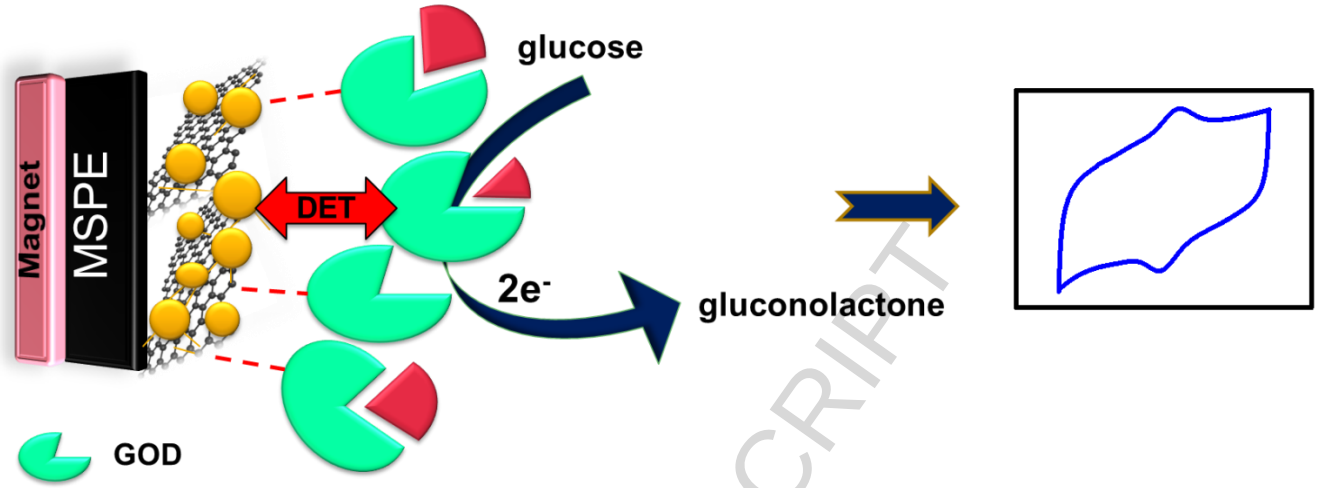

Highlights

- The RGO-Fe_3O_4/GOD nanocomposite was entrapped on MSPE by magnetic field.
- Glucose oxidase immobilized on RGO-Fe_3O_4 via electrostatic interaction without a binder.
- A stable and highly selective of glucose biosensor based on direct electron transfer.
- The biosensor could avoid the possible interferences.